ELSEVIER

PII: S0032-3861(97)00573-9

Polymer Vol. 39 No. 12, pp. 2657–2664, 1998
© 1998 Elsevier Science Ltd
Printed in Great Britain. All rights reserved
0032-3861/98/$19.00+0.00

Acid–base properties of poly(propylene imine) dendrimers

René C. van Duijvenbode[a], Michal Borkovec[b] and Ger J. M. Koper[a,*]
[a]*Leiden Institute of Chemistry, Leiden University, Gorlaeus Laboratories, PO Box 9502, 2300 RA Leiden, The Netherlands*
[b]*Federal Institute of Technology, ETH-ITO, Grabenstrasse 3, 8952 Schlieren, Switzerland*
(Accepted 8 July 1997)

Potentiometric titration experiments of poly(propylene imine) dendrimers (up to the fifth generation) were carried out at salt concentrations of 0.1, 0.5 and 1.0 M KCl and NaCl. The experiments were performed at two different locations on different instruments and were converted to titration curves using two different methods, resulting in a consistent experimental data set for the dendrimers measured. The titration curves feature two distinct steps around p*H* 6 and 10 with an intermediate plateau at 2/3 of the total ionizable groups. This protonation pattern reflects short-ranged repulsive interactions between ionizable sites and can be modeled using an Ising model with nearest-neighbour pair interactions. The intermediate plateau results from the stability of an onion-like structure where all odd shells of the dendrimer are protonated, while the even ones remain deprotonated. The Ising model permits a quantitative analysis of the titration curves. For larger dendrimers, this Ising approach is shown to be superior to the classical analysis in terms of successive protonation equilibria. © 1998 Elsevier Science Ltd. All rights reserved.

(Keywords: dendrimer; potentiometric titration; Ising model)

INTRODUCTION

New kinds of hyperbranched molecules, which are also refered to as dendrimers or starburst-polymers (recently introduced as *Astramol® dendrimers*), have been synthesized and their unusual properties have sparked many potential applications ranging from organic synthesis to medical sciences[1–5]. The synthesis of such molecules begins with a central reactive unit and proceeds through repetitive reaction cycles of an appropriate monomeric unit with the core. This procedure leads to consecutive generations of globular dendrimers. An example of this sequence is shown for 1,4-diaminobutane poly(propylene imine) dendrimers in *Figure 1*. These dendrimers, which will be abbreviated as DAB-dendr-$(NH_2)_x$ in the following, are characterized by x, the number of primary (terminal) amine groups in the outermost shell. The synthetic route starts from 1,4-diaminobutane to which four propylene imine monomers are added. This represents the first generation of the dendrimers ($x = 4$). Stepwise additions of propylene imine monomers lead to dendrimers up to the fifth generation ($x = 8$, 16, 32, 64). Packing constraints within the outermost shells make the complete synthesis of higher generations impossible.

Physico-chemical properties of such dendrimers are sometimes in sharp contrast to the behaviour of linear polymers. For example, the specific viscosity of dendrimer solutions goes through a maximum as a function of the molecular weight, while for linear polymers this quantity is monotonically increasing[4]. This behaviour, which is typical for dendrimers, is related to their highly branched structure, which makes these molecules much more compact than linear polymers. In this paper we shall demonstrate that the acid–base properties of dendrimers show characteristic differences to the linear analogues as well.

The features of acid–base properties for weak linear polyelectrolytes are well-studied[6–10]. The protonation of a linear polyelectrolyte with one kind of ionizable group typically proceeds in two steps; an intermediate plateau in the titration curve appears at half protonation. This plateau is related to a stable intermediate protonation state, where protonated and deprotonated groups alternate along the chain. The stability of this state is caused by the short-range character of the interaction potential between ionizable sites. This interaction potential is dominated by the crossover between strong Coulomb repulsion in the low dielectric constant backbone, which acts at small separations, and a weak screened Coulomb potential in the electrolyte, which is operational at larger separations. The presence of this crossover leads to a very rapid decay of the interaction potential between two charged groups on the polymer backbone[11]. For this reason, only nearest-neighbour sites, which are connected by carbon chains, interact strongly. With such short-range interactions, the system can greatly reduce its electrostatic energy by ionizing every second site. The splitting between the two protonation steps is related to the interaction energy of forming a nearest-neighbour pair of ionized sites. Compared to the splitting between the two protonation steps of the corresponding diprotic acid, the splitting is roughly twice as large because in the linear polyelectrolyte, each site has two nearest neighbours and only one in the latter case.

All these effects can be quantitatively treated in the framework of the Ising model[6–13]. For each site, this model introduces a state variable, which is either zero or one, depending on whether the site is deprotonated or

* To whom correspondence should be addressed

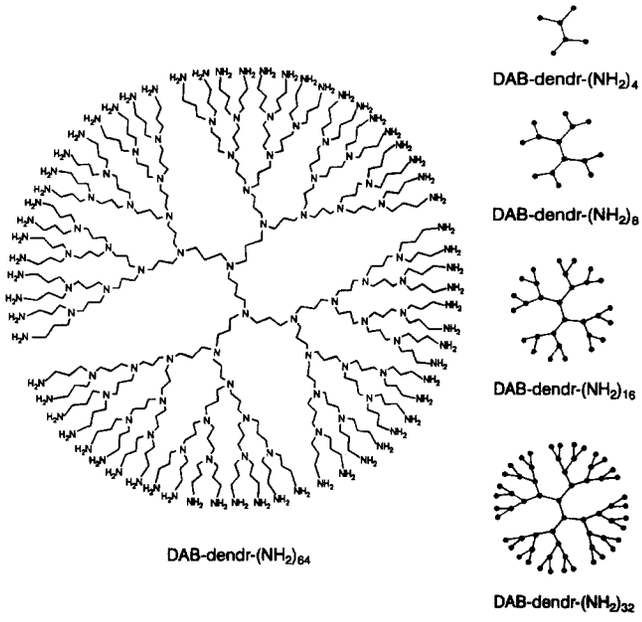

Figure 1 Molecular structure of the 1,4-diaminobutane poly(propylene imine) dendrimer DAB-dendr-$(NH_2)_{64}$ and schematic representations of the smaller generations DAB-dendr-$(NH_2)_4$, DAB-dendr-$(NH_2)_8$, DAB-dendr-$(NH_2)_{16}$ and DAB-dendr-$(NH_2)_{32}$

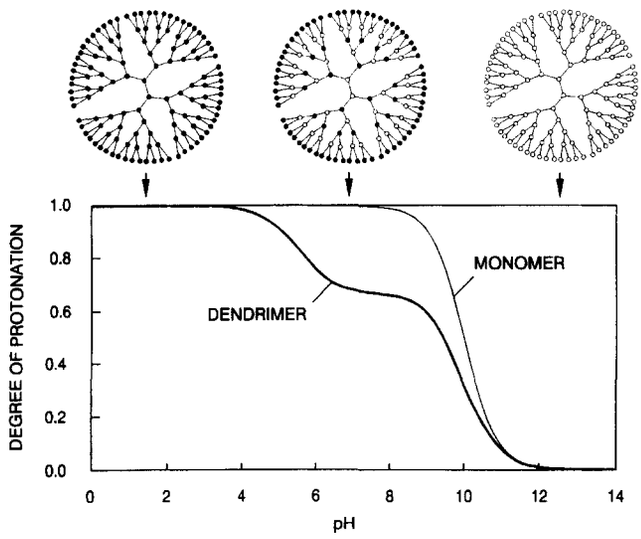

Figure 2 Calculated titration curve for a simplified Ising model of DAB-dendr-$(NH_2)_{64}$ for identical ionizable groups. For the dendrimer the parameters are microscopic $p\hat{K} = 10$ and the pair interaction parameter $\epsilon = 1.5$ (thick line). The corresponding most important protonation microstates are also shown (top). The titration curve for the monomer with $p\hat{K} = 10$ is given for comparison (thin line). The two step protonation curve results from the stability of the intermediate onion-like protonation state, where 2/3 of the sites are protonated. The splitting between both protonation steps on the pH axis is 3ϵ

protonated. The free energy of various ionization microstates is expressed in terms of these state variables and involves microscopic ionization constants and pair interaction energies. The titration curve (and other quantities of interest) can be calculated from appropriate thermal averages of this free energy. The linear chain with nearest-neighbour pair interactions can be solved analytically. This simple model is able to represent the titration curves of linear polyelectrolytes in an approximate fashion[14]. A better description may be obtained when including higher order interactions, in particular triplet interactions[10]. The resulting titration curve shows two distinct protonation steps with the intermediate plateau at half protonation.

As will be shown in detail below, the same principles govern the protonation behaviour of dendrimers. As in the case of linear polyelectrolytes, interactions between the ionizable sites can be assumed, to a good degree of approximation, to be short ranged and to act along the carbon chains only. Due to the highly branched structure of the dendrimer, two main differences between the protonation behaviour of the dendrimers and the corresponding linear polyelectrolytes emerge: (i) the intermediate plateau in the titration curve of a dendrimer arises at a degree of protonation of 2/3 and corresponds to alternating shells of protonated and deprotonated sites (see *Figure 2*); (ii) since every dendrimer site has three nearest neighbours, the overall effect of interactions is much stronger for the dendrimer than for the linear polyelectrolyte. The splitting between the two protonation steps is now three times larger than the splitting between the two protonation steps of the corresponding diprotic acid or base. The effects of interactions will thus be more pronounced for dendrimers than for the linear analogues.

Again, all these effects can be quantified on the basis of the Ising model with nearest-neighbour interactions. For the dendrimer, however, one has to consider the appropriate tree-like arrangement of the ionizable sites on the branched dendrimer structure. (In statistical mechanics literature, this arrangement is referred to as the Cayley-tree[15].) Unfortunately, even in the simplest case of nearest-neighbour interactions, a simple analytical solution no longer exists. For such tree-like structures, however, very efficient numerical techniques are available and one can readily calculate the corresponding titration curves[11]. A typical result of such a calculation is given in *Figure 2*. The resulting titration curve shows two distinct protonation steps, but in contrast to the linear polyelectrolyte, the intermediate plateau occurs at a degree of protonation of 2/3.

In the present paper, we shall focus on results from potentiometric titration experiments for DAB-dendr-$(NH_2)_x$ with $x = 4$, 8, 16, 32 and 64. The titration data are quantitatively analyzed in terms of the Ising model with nearest-neighbour pair interactions. Thereby, one must consider the fact that the proton affinities of the various shells and the pair interactions between them may differ. With this slightly generalized Ising model, the entire set of titration data for dendrimers up to DAB-dendr-$(NH_2)_{64}$ can be rationalized.

The dendrimer titration curves were also analyzed in terms of successive protonation equilibria. This approach requires the determination of all macroscopic dissociation constants. As the number of these constants equals the number of ionizable sites, this method is only applicable if this number is not too large. In the present case, we have found this classical procedure to be meaningful for DAB-dendr-$(NH_2)_4$ and DAB-dendr-$(NH_2)_8$, which have 6 and 14 ionizable sites, respectively. For larger dendrimers, however, the number of sites (and the number of adjustable parameters) quickly becomes so large that the classical approach in terms of successive protonation equilibria is no longer feasible. For the Ising model, on the other hand, the number of adjustable parameters always remains small, but the size of the dendrimer is practically unlimited.

ISING MODEL OF POLYPROTIC SYSTEMS

General formulation

Let us summarize how ionization equilibria in polyprotic systems can be rationalized using the Ising model[10,13–17]. In this model, the protonation microstate is characterized by a set of state variables $s_1,\ldots,s_N$, where $s_i = 0$ if the site i is deprotonated and $s_i = 1$ if it is protonated (N is the total number of ionizable sites). Including pair interactions only, the free energy of a given protonation state F relative to the completely deprotonated state can be written as

$$\frac{F(s_1,\ldots,s_N)}{kT\ln 10} = \sum_i (\mathrm{p}H - \mathrm{p}\hat{K}_i)s_i + \sum_{i<j} \epsilon_{ij}s_is_j \qquad (1)$$

where kT denotes thermal energy. In this equation we have introduced the following abbreviations: pH is the negative common logarithm of the proton activity (in M), p$\hat{K}_i$ the negative common logarithm of the microscopic dissociation constant of site i given all other groups are deprotonated, and $\epsilon_{ij} > 0$ characterizes the strength of the pair interactions between sites i and j. The factor of ln 10 on the left hand side of equation (1) is introduced in order to facilitate the comparison of the pair interaction parameters with the pH scale. For the present developments, we shall assume that the pair interaction parameters ϵ_{ij} are nonzero for nearest neighbours only.

Titration curve

All system properties can be obtained from the grand partition function

$$\Xi = \sum_{s_1,\ldots,s_N} \mathrm{e}^{-F(s_1,\ldots s_N)/(kT)} \qquad (2)$$

The classical potentiometric titration curve, which represents the average degree of protonation θ as a function of pH, is given by

$$\theta = \frac{z}{N}\frac{\partial \ln \Xi}{\partial z} \qquad (3)$$

where z is the activity of the protons (p$H = -\log_{10} z$). The classical description in terms of macroscopic ionization constant is recovered from the Ising model by realizing that equation (2) can be written as a polynomial in the activity, i.e.

$$\Xi = \sum_{n=0}^{N} \bar{K}_n z^n \qquad (4)$$

where the coefficients $\bar{K}_n$ are just the macroscopic formation constants of the molecule with n protons bound ($\bar{K}_0 = 1$). Inserting equation (4) into equation (3) the familiar expression of the titration curve of a polyprotic molecule is obtained

$$\theta = \frac{1}{N}\frac{\sum_{n=0}^{N} n\bar{K}_n z^n}{\sum_{n=0}^{N} \bar{K}_n z^n} \qquad (5)$$

The commonly used macroscopic pK values are given by $\mathrm{p}K_n = \log_{10} K_n$ where $K_n = \bar{K}_{n-1}/\bar{K}_n$ are the stepwise dissociation constants.

Numerical implementation

For smaller molecules, the partition function of the Ising model, or equivalently the macroscopic formation constants, can be evaluated from equation (2) by direct enumeration[13]. As the number of sites becomes larger (typically $N > 25$), the direct enumeration technique becomes computationally prohibitively expensive. Various methods are available for the treatment of larger systems, but in the present case of dendrimers, the most efficient scheme relies on numerical evaluation of exact recursion relations. This method makes use of the particular tree-like structure of the dendrimer, and of the fact that only nearest-neighbour interactions within the carbon chains are operational. These assumptions pose no restriction in the present case, and we can thus evaluate the titration curves efficiently for dendrimers of any size of interest. The details of the numerical implementation are given elsewhere[18].

A sample result of such a calculation for the DAB-dendr-$(NH_2)_{64}$ molecule is shown in *Figure 2*. For simplicity, all sites are assumed to be equivalent. Thus we take $\mathrm{p}\hat{K}_i = \mathrm{p}\hat{K} = 10$ for all sites and for all nearest-neighbour interaction parameters a common value of $\epsilon = 1.5$. The presence of these interactions makes the titration curve of the dendrimer significantly different from the titration curve of the monomeric analogue (a simple base with p$\hat{K} = 10$). The typical shape of the dendrimer titration curve can be understood as follows. In the first protonation step near pH = p$\hat{K}$, the sites protonate without influencing each other. However, as the degree of protonation of $\theta = 2/3$ is approached, only the odd shells start to protonate while the even shells remain deprotonated (see *Figure 2*). In this way, the system avoids the formation of nearest-neighbour pairs which are energetically unfavourable. Protonation beyond $\theta = 2/3$ will necessarily involve sites where three nearest-neighbour pair interactions must be overcome. Thus, the second protonation step happens near p$H = \mathrm{p}\hat{K} - 3\epsilon$.

This simple picture captures the protonation mechanism of dendrimers semi-quantitatively. In the real situation, however, the proton affinities of the individual shells are different, and not all pair interactions have the same strength. Such features will be inferred from the analysis of experimental data.

EXPERIMENTAL

Materials

The Astramol™ (DSM, The Netherlands) dendrimers DAB-dendr-$(NH_2)_x$ (x = 4, 8, 16, 32 and 64) were used as received. Sample numbers were 4pa – 1, 8pa – 2, 16pa – 1c, 16pa – 1cc, 32pa – 1, 32pa – 1cc, 64pa – 1 and pa64 – n912351. The sample 64pa – 1, has a higher cobalt concentration (500 ppm, according to specifications which are based on X-ray measurements) than the sample pa64 – n912351 (5 ppm).

The carbon and nitrogen contents of these compounds were independently checked using a CHNS-elemental analyser (Heraeus).

The titrations were performed with HCl (Titrisol; Merck), NaOH/KOH (Merck) and the supporting electrolyte NaCl/KCl of analytical grade (Merck). All solutions were prepared with boiled water from a high quality water purification system and kept under nitrogen. Carbonate-free base was obtained from a cooled and centrifuged 50%

solution of KOH and NaOH[19]. Accurate concentrations of the acid and base were checked against potassium hydrogen phthalate. All titrations were carried out at 25 ± 1°C.

Potentiomentric titrations

The potentiometric titrations were carried out at two different instruments: one at the Leiden University, *Leiden*, and one at the Swiss Federal Institute of Technology in Zurich, *Zurich*. The Leiden instrument involved a computer controlled Radiometer 11 titrator (Radiometer, Copenhagen) equipped with an ABU 13 automatic burette and an HI 1131 glass electrode with an HI 8417 p*H* meter (Hanna Instruments, Italy). The ionic strength of the samples was kept constant by using acid and base solutions at the same ionic strength as the sample itself. The electrodes were calibrated with standard buffer solutions.

The Zurich instrument was a commercial, high-precision computer controlled titration apparatus[20], which utilizes a separate glass electrode and an Ag/AgCl reference electrode with a salt bridge. The fully automated set-up involves four burettes with the following solutions: (1) standardized carbonate-free 0.05 M NaOH or KOH; (2) standardized 0.05 M HCl; (3) 2.0 M KCl or NaCl; and (4) pure water. Calibration of the electrodes was performed by means of titrations of pure electrolyte solutions. The measured potential differences as a function of the volume of added base or acid were used to fit electrode parameters including terms to correct for the diffusion potential[21]. Activity coefficients derived from the fitting procedure were in good agreement with literature values.

Each titration cycle consisted of a forward titration of an acidified sample at given ionic strength and a backward titration with acid. For each titration point, a given amount of base or acid was added and, in the case of the Zurich instrument, the ionic strengths were adjusted accordingly with appropriate amounts of the salt solution or water. Each point was equilibrated until the potential drift was below 0.03 mV per minute. Approximately 100 titration points were recorded for the entire titration cycle. Three titration cycles were performed at 0.1, 0.5 and 1.0 M. A single experimental run consisted of a set of forward and backward titrations for these three ionic strengths on the same sample, each lasting about 6 h. The dendrimer titrations were carried out at concentrations around 100 mM of the amine groups (total nitrogen content). All titrations were repeated twice to confirm reproducibility. The titration data obtained from both instruments was the same within experimental error.

To obtain the titration curve of the degree of protonation *versus* p*H* from the measured data, which consists of the p*H* *versus* the added volume of acid or base, two methods were used. The first method explicitly uses the electroneutrality condition

$$\theta = \frac{(c_a - c_b) - c_{H^+} + c_{OH^-}}{c_p} \qquad (6)$$

with c_a the concentration of added acid and c_b the concentration of added base so that $c_a - c_b$ is the equivalent concentration of net (single valenced) acid added and c_{H^+} and c_{OH^-} are the concentrations of free H^+ and free OH^- in mol/l as determined by the p*H* of the solution. In order to convert the measured p*H* values into proton and hydroxide concentrations, two activity coefficients were introduced. These coefficients could be determined directly from the experimental data by requiring the slopes of the titration curve, of degree of protonation *versus* p*H*, to be horizontal at both the high and the low limiting values of p*H*. Activity coefficents derived from this procedure were, within experimental error, in agreement with the literature values.

In the second method, the degree of protonation as a function of p*H* was obtained by subtracting the titration curve of the dendrimers from the blank titration curve of the pure electrolyte solution with the same ionic strength. The total nitrogen content of the sample is used for normalization. Both methods gave reliable results, the latter slightly more accurate with, in the p*H* range from 3 to 11, an error of ± 0.05 on the p*H* scale and an error of $\pm 10^{-2}$ in the degree of protonation.

Data analysis

The predictions of the Ising model with nearest-neighbour pair interactions were fitted to the experimental titration curves with a non-linear least-squares procedure. The fitting parameters were the microscopic p*K* values of the individual shells and the corresponding pair interaction parameters. Due to the limited number of parameters, the parameter estimation was possible for all dendrimers investigated.

The ionization constants were obtained from the titration curves as successive dissociation constants by fitting equation (5) to the experimental data by means of a similar non-linear least-squares procedure. A reliable determination of all successive dissociation constants was only possible for DAB-dendr-$(NH_2)_4$ and DAB-dendr-$(NH_2)_8$. For the higher dendrimers the least-squares problem did contain too many unknown parameters.

The overall consistency of the experiments and data analaysis was checked by titrating ethylene diamine and citric acid. The titration curves were fitted to equation (5) with $N = 2$ and 3, respectively. The obtained p*K* values of these compounds were within 0.08 p*K* units of the literature values[22].

RESULTS

Experimental titration data

The titration curves of the largest dendrimer DAB-dendr-$(NH_2)_{64}$ are shown in *Figure 3* for KCl concentrations of 0.1, 0.5 and 1.0 M. The curves do show the expected two step behaviour, with the intermediate plateau near $\theta = 2/3$. Increasing the ionic strength causes the titration curves to shift to higher p*H* values.

Results of three different test experiments, which were performed to confirm the internal consistency of the data, are also shown in *Figure 3*. At an ionic strength of 1.0 M, the results of a forward and a backward titration are compared. The lack of any hysteresis shows that equilibrium has been achieved and verifies the present titration procedures. At an ionic strength of 0.1 M, titration curves at two initial dendrimer concentrations (8 and 80 mM nitrogen) are compared. The coincidence of these two curves reveals that the dendrimer concentration in the titration experiments was sufficiently low. Therefore, all interactions between dendrimers can be neglected and the dendrimers can be treated independently. Also at an ionic strength of 0.1 M, two different cations Na^+ and K^+ are compared (see the inset in *Figure 3*). The titration curves coincide except in the high p*H* range (above p*H* 10), where

the so-called alkali error of the electrode system interfered[23].

Different samples of the highest generation yielded almost the same curve. With the same 64pa – 1, with the higher cobalt concentration, irreversibility occurred in the basic regions down to pH = 8. The sample pa64-n912351, with the lower cobalt concentration, yielded a fully reversible titration curve as shown in *Figure 3*. A possible explanation for the irreversibility at higher cobalt content is that the cobalt ions induce clustering of the dendrimers in the basic regime. This effect is expected to affect the acid titrations more strongly than the base titrations.

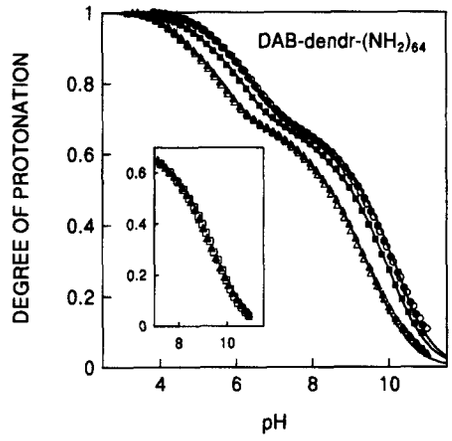

Figure 3 Experimental titration curves of the poly(propylene imine) dendrimer DAB-dendr-$(NH_2)_{64}$ at a concentration of 80 mM of nitrogen plotted as the degree of protonation θ *versus* pH in KCl as background electrolyte. The ionic strengths are 0.1 (▲), 0.5 (■) and 1.0 M (●). Smaller dendrimer concentration of 8 mM nitrogen is shown for an ionic strength of 0.1 M (△). The backward titration curve with acid is shown for an ionic strength of 1.0 M (○). Solid lines are best fits with the Ising model with the parameters shown in *Table 1*. In the inset, the effect of different cations, Na^+ (□) and K^+ (▲), is shown for ionic strength of 0.1 M

Figure 4a–d summarize the experimental titration curves for the smaller dendrimers. The titration curves for different generations have a rather similar appearance. We have also observed reversibility for these titration curves. It was further confirmed that the dendrimer concentration was sufficiently low to treat the dendrimers independently.

Interpretation with the Ising model

The solid lines in *Figures 3 and 4* are least-squares fits to the Ising model with nearest-neighbour pair interactions. One observes that the Ising model is able to model the titration curves for the different dendrimers sufficiently well. (For DAB-dendr-$(NH_2)_4$ the fit is less good, see below.) In order to obtain fits of this quality, it is essential to assume different pK values for the different shells and different pair interaction parameters. If all pK values and pair interaction parameters are taken to be equal, the shape of the calculated curve is in semi-quantitative agreement with experiment (cf. *Figure 2*), but the quality of the fit is poor.

The simplest Ising model with nearest-neighbour pair interactions, which is able to describe the experimental data in a satisfactory fashion, involves four different microscopic pK values and three nearest-neighbour pair interaction parameters, see *Figure 5*. The microscopic pK values are denoted by $p\hat{K}^{(1)}$, $p\hat{K}^{(3,o)}$, $p\hat{K}^{(3)}$ and $p\hat{K}^{(3,i)}$. The outermost primary amines have the values $p\hat{K}^{(1)}$. We have three groups of tertiary amines. The outermost shell

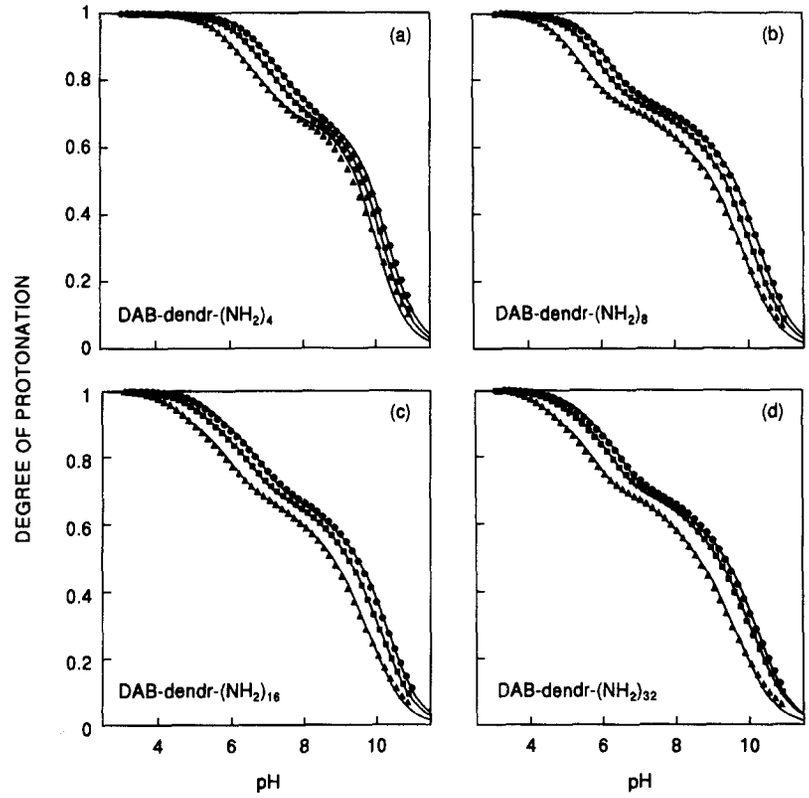

Figure 4 Experimental titration curves of the smaller poly(propylene imine) dendrimers at a concentration of 80 mM of nitrogen plotted as the degree of protonation θ *versus* pH in KCl as background electrolyte. (a) DAB-dendre-$(NH_2)_4$; (b) DAB-dendr-$NH_2)_8$; (c) DAB-dendr-$(NH_2)_{16}$; and (d) DAB-dendr-$(NH_2)_{32}$. The ionic strengths are 0.1 (▲), 0.5 (■) and 1.0 M (●). Solid lines are best fits with the Ising model with the parameters shown in *Table 1*

Table 1 Ising model parameters for different dendrimers of generation k and at ionic strength I

I[M]	k	x	N	$p\hat{K}^{(3,i)}$	$p\hat{K}^{(3)}$	$p\hat{K}^{(3,o)}$	$p\hat{K}^{(1)}$	ϵ_1^a	ϵ_2^a	ϵ_3
	1	4	6	9.02	–	–	9.97	0.61	1.05	–
	2	8	14	8.19	–	9.66	9.85	0.61	1.05	1.57
0.1	3	16	30	8.19	7.99	9.72	9.79	0.61	1.05	1.57
	4	32	62	8.19	8.02	9.71	9.70	0.61	1.05	1.57
	5	64	126	8.19	7.95	9.66	9.56	0.61	1.05	1.57
	1	4	6	9.41	–	–	10.14	0.59	1.03	–
	2	8	14	8.82	–	9.91	10.12	0.59	1.03	1.46
0.5	3	16	30	8.82	8.54	9.96	10.13	0.59	1.03	1.46
	4	32	62	8.82	8.59	10.00	10.15	0.59	1.03	1.46
	5	64	126	8.82	8.47	9.93	10.05	0.59	1.03	1.46
	1	4	6	9.57	–	–	10.29	0.56	0.97	–
	2	8	14	9.07	–	9.64	10.33	0.56	0.97	1.21
1.0	3	16	30	9.07	8.75	9.72	10.34	0.56	0.97	1.21
	4	32	62	9.07	8.74	9.67	10.29	0.56	0.97	1.21
	5	64	126	9.07	8.72	9.67	10.25	0.56	0.97	1.21

[a]Taken from Ref. 13 and not varied

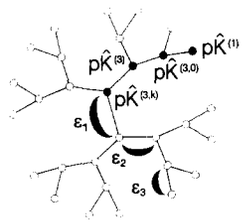

Figure 5 Schematic representation of a dendrimer molecule showing the various parameters used to fit the Ising model prediction to the experimental curves

Table 2 Comparison of macroscopic pK_n values for DAB-dendr-$(NH_2)_4$ at different ionic strengths

I[M]	0.1		0.5		1.0	
n	Fit[a]	Ising[b]	Fit[a]	Ising[b]	Fit[a]	Ising[b]
1	10.83	10.60	11.02	10.78	10.93	10.93
2	10.22	10.16	10.40	10.33	10.58	10.48
3	9.72	9.79	10.00	9.96	10.06	10.11
4	9.13	9.35	9.41	9.52	9.56	9.67
5	7.16	7.20	7.65	7.62	7.91	7.90
6	6.01	6.01	6.51	6.46	6.77	6.76

[a] Obtained by direct fitting of experimental data with an accuracy of ± 0.05

[b] Calculated from the Ising model parameters given in *Table 1*

of tertiary amine groups has $p\hat{K}^{(3,o)}$, the two innermost tertiary amines $p\hat{K}^{(3,i)}$, while all the remaining ones $p\hat{K}^{(3)}$. The three pair interaction parameters are abbreviated as ϵ_1, ϵ_2 and ϵ_3. The outermost bonds between primary and tertiary amines have the value ϵ_3. The innermost bond, which consists of four carbons, has the value ϵ_1. All remaining bonds have the value ϵ_2.

The resulting parameter values are given in *Table 1*. They were estimated according to the following procedure. The pair interaction parameters ϵ_1 and ϵ_2 were estimated from macroscopic pK values of linear amines[13] and were not adjusted further. Thus each dendrimer involves five adjustable parameters at maximum. The titration curves of DAB-dendr-$(NH_2)_4$ were fitted by adjusting two parameters $p\hat{K}^{(1)}$ and $p\hat{K}^{(3,i)}$. One observes that the tertiary group is slightly more acidic than the primary one. The titration curve of DAB-dendr-$(NH_2)_8$ can be rationalized by introducing two additional parameters; $p\hat{K}^{(3,o)}$ in order to account for a smaller proton affinity of the middle shell and by assuming a larger interaction parameter ϵ_3 for the outermost shell. The parameters $p\hat{K}^{(3,i)}$ and ϵ_3 determined from DAB-dendr-$(NH_2)_8$ will be used for all higher dendrimers. The titration curve for DAB-dendr-$(NH_2)_{16}$ can be fitted by introducing one additional parameter $p\hat{K}^{(3)}$ which reflects the different proton affinity of the first shell from the inside. The titration curves for DAB-dendr-$(NH_2)_{32}$ and DAB-dendr-$(NH_2)_{64}$ can be explained with the same model using equal values of $p\hat{K}^{(3)}$ for all additional shells within a single dendrimer. In spite of the fact that at maximum five parameters are determined from a single titration curve, these parameters remain remarkably constant throughout all generations investigated. The only exception is $p\hat{K}^{(1)}$ at 0.1 M, which shows a systematic variation with generation number. This variation will be explained further below. Thus the present model captures the intrinsic features of the dendrimer protonation sequence.

Note that only DAB-dendr-$(NH_2)_4$ does not fit into the scheme as well as all the others. The present scheme is not sufficiently flexible and does not allow a better fit of its titration curve than the one shown in *Figure 4a*, but since this molecule represents the first generation in the whole series of dendrimers, we are not particulary concerned with minor deficiencies of the model for this particular molecule.

Classical interpretation with polyprotic equlibria

For comparison, the titration of DAB-dendr-$(NH_2)_4$ and DAB-dendr-$(NH_2)_8$ were analyzed in terms of classical polyprotic equilibria. The titration curves were fitted with equation (5). The resulting fits were essentially perfect in all cases.

The obtained macroscopic pK values are summarized in *Table 2–Table 3*. These values are expected to be accurate within ± 0.05. These fitted values are further compared with the corresponding macroscopic pK values of the Ising model which were calculated with the parameters given in *Table 1*. For DAB-dendr-$(NH_2)_4$ with its six ionizable sites, the macroscopic pK values are readily determined by any least-squares procedure and agree well with the values obtained from the Ising model (see *Table 2*). For

Table 3 Comparison of macroscopic pK_n values for DAB-dendr-$(NH_2)_8$ at different ionic strengths

I[M]	0.1		0.5		1.0	
n	Fit[a]	Ising[b]	Fit[a]	Ising[b]	Fit[a]	Ising[b]
1	11.21	10.88	11.11	11.14	11.85	11.28
2	10.50	10.49	10.91	10.76	11.23	10.91
3	10.49	10.22	10.50	10.49	10.80	10.66
4	9.88	9.98	10.29	10.25	10.61	10.45
5	9.88	9.75	10.09	10.03	10.36	10.25
6	9.40	9.51	9.79	9.80	10.09	10.05
7	9.25	9.25	9.60	9.56	9.86	9.82
8	8.85	8.93	9.26	9.27	9.61	9.54
9	8.36	8.35	8.85	8.85	9.17	9.11
10	7.58	7.38	8.09	7.96	8.61	8.24
11	6.18	6.15	6.70	6.61	7.21	6.89
12	5.56	5.66	6.11	6.14	6.34	6.43
13	5.20	5.22	5.78	5.73	6.14	6.03
14	4.68	4.70	5.17	5.24	5.44	5.55

[a] Obtained by direct fitting of experimental data
[b] Calculated from the Ising model parameters in *Table 1*

DAB-dendr-$(NH_2)_8$ with its 14 ionizable sites, one must fit the same number of macroscopic pK values, which cannot be meaningfully done without introducing the constraint $pK_{n+1} \leq pK_n$ into the fitting procedure. However, a general agreement between the fitted values and those obtained from the Ising model can be observed.

At this point, the basic advantage of the Ising model description over the classical description in terms of macroscopic protonation equilibria becomes evident. For DAB-dendr-$(N_2)_8$ the Ising model involves six parameters (including the ones which are not fitted), while the classical polyprotic equilibrium model involves 14. For the next generation DAB-dendr-$(NH_2)_{16}$, the Ising model requires seven parameters, while it is no longer meaningful to fit 30 macroscopic pK values from the titration curve. Clearly, the larger the dendrimer, the more extreme the situation becomes. For DAB-dendr-$(NH_2)_{64}$ the classical description would call for 126 macroscopic pK values, while for the Ising model seven parameters still suffice.

DISCUSSION

Potentiometric titration experiments of poly(propylene imine) dendrimers have been performed for salt concentrations of 0.1, 0.5 and 1.0 M and two different types of cations (Na^+ and K^+). The experiments have been performed at two different locations on different instruments and have been converted to titration curves using two different methods. The result of this concerted action is a consistent experimental data set for the dendrimers measured.

The titration experiments reveal a characteristic protonation curve with two protonation steps around pH values of 6 and 10 with an intermediate plateau where 2/3 of the ionizable sites are protonated (see *Figures 3 and 4*). This protonation pattern reflects short-ranged repulsive interactions between neighbouring sites and can be captured with a simple Ising model where all interactions between equivalent sites are assumed to be the same. The result of such a model calculation, which reveals the same characteristics as the experimental data, is shown in *Figure 2*. The intermediate plateau results from the stability of an onion-like structure where all odd shells are protonated, while the even ones are deprotonated.

A quantitative interpretation of the titration data is also possible with the Ising model with nearest-neighbour pair interactions but one must allow for different pK values of the different shells, as well as different pair interaction parameters for the outermost and innermost bonds (see *Table 1*). The fact that the pair interaction parameter is larger for the outermost shell than for the remaining ones is probably related to a better solvation of these bonds. The pK values of the various shells are in line with the observation that primary amine groups are more basic than tertiary ones[24]. The fact that the innermost amine groups are more acidic probably related to its different coordination which involves a butyl chain instead of a propyl chain. The differences between the pK values of the amine groups between the outermost shell and the ones further inside must again be related to solvation effects. Note, however, that all determined parameters remain remarkably constant throughout all generations investigated and thus reflect intrinsic features of the protonation process. The only parameter which systematically varies with the generation number, is $p\hat{K}^{(1)}$ at 0.1 M. This parameter decreases with increasing size of the dendrimer. Such pK shifts are induced most likely by neighbouring amine groups, which are situated on different chains. Such effects have been observed for other amines at lower ionic strength as well[22]. For higher ionic strengths, the screening is more effective and these effects disappear.

The Ising model can be interpreted in terms of the classical stepwise protonation constants as well. Provided the number of ionizable sites is not too large, these macroscopic pK values can be directly determined from titration data. This comparison was carried out for the two smallest dendrimers. The macroscopic pK values derived from direct fitting of the titration data agree favourably with the values calculated from the Ising model. For the larger dendrimers, the classical approach with stepwise protonation is no longer practical, since a large number of fitting paramaters is involved. A meaningful interpretation can only rely on the Ising model.

While we did exclusively focus on poly(propylene imine)

dendrimers, the concepts developed here are expected to be applicable more generally. For other types of ionizable dendrimers similar analogous protonation patterns are expected.

REFERENCES

1. Bielinska, A., Kukowska-Latallo, J. F., Johnson, J., Tomalia, D. A. and Baker, J. R. Jr, *Nucleic Acids Research*, 1996, **24**, 2176.
2. Haensler, J. and Szoka, F. C. Jr, *Bioconjugate Chemistry*, 1993, **4**, 372.
3. Knapen, J. W. J., van der Made, A. W., de Wilde, J. C., van Leeuwen, P. W. N. M., Wijkens, P., Grove, D. M. and van Koten, G., *Nature*, 1994, **372**, 659.
4. Tomalia, D. A. and Durst, H. D., *Topics in Current Chemistry*, 1993, **165**, 193.
5. Frechet, J. M. J., *Science*, 1994, **263**, 1710.
6. Marcus, R. A., *J. Phys. Chem.*, 1954, **58**, 621.
7. Katchalsky, A., Mazur, J. and Spitnik, P., *J. Polym. Sci.*, 1957, **23**, 513.
8. Kitano, T., Kawaguchi, S., Ito, K. and Minakata, A., *Macromolecules*, 1987, **20**, 1598.
9. Kawaguchi, S., Kitano, T., Ito, K. and Minakata, A., *Macromolecules*, 1990, **23**, 731.
10. Smits, R. G., Koper, G. J. M. and Mandel, M., *J. Phys. Chem.*, 1993, **97**, 5745.
11. Borkovec, M. and Koper, G. J. M., *Macromolecules*, 1997, **30**, 2151.
12. Harris, F. E. and Rice, S. A., *J. Phys. Chem.*, 1954, **58**, 725.
13. Borkovec, M. and Koper, G. J. M., *J. Phys. Chem.*, 1994, **98**, 6038.
14. Borkovec, M. and Koper, G. J. M., *Ber. Bunsenges. Phys. Chem.*, 1996, **100**, 764.
15. Baxter, R. J., *Exactly Solved Models in Statistical Mechanics*. Academic Press, New York, 1982.
16. Borkovec, M., Rusch, U., Cernik, M., Koper, G. J. M. and Westall, J. C., *Colloids and Surfaces A*, 1996, **107**, 285.
17. Koper, G. J. M. and Borkovec, M., *J. Chem. Phys.*, 1996, **104**, 4204.
18. Borkovec, M., Daicic, J. and Koper, G. J. M., *Proc. Natl. Acad. Sci.* 1997, in press.
19. Vogel, A.I., *A Text-book of Quantitative Inorganic Analysis*, 3rd edn. Longmans, London, 1961.
20. Kinniburgh, D. G., Milne, C. J. and Venema, P., *Soil Sci. Soc. Am. J.*, 1995, **59**, 417.
21. Baes, C. F. and Mesmer, R. E., *The Hydrolysis of Cations*. Krieger Publishing Company, Malabar, FL, 1986.
22. Smith, R. M. and Martell, A. E., *Critical Stability Constants*. Plenum Press, New York, 1989.
23. Galster, H., *pH Measurement*. VCH Publishers, Inc., New York, 1991.
24. Perrin, D. D., Dempsey, B. and Serjeant, E. P., *pK_a Prediction for Organic Acids and Bases*. Chapman and Hall, London, 1981.